

# Synthesis and characterization of activated carbon spheres SILP catalysts for the selective hydrogenation of aldehydes using a well-defined Fe(II) PNP complex

Rafael Amorim Leandro de Castro Amoedo

*Centro de Química Estrutural, Departamento de Engenharia Química, Instituto Superior Técnico, Lisbon, Portugal*

*Institute of Applied Synthetic Chemistry, Vienna University of Technology, Vienna, Austria*

ARTICLE INFO	ABSTRACT
<i>Date:</i> November 2017	Supported Ionic Liquid Phase (SILP) systems are in a crescendo development, since they are able to provide the benefits of both homogeneous and heterogeneous catalysis, contributing to the increasing demand for cleaner processes. In this work, activated carbon based SILP systems using a newly developed Fe(II) PNP complex were synthesized for the hydrogenation of 4-Fluorobenzaldehyde. Full conversion was achieved after 2h, with TON and TOF values up to 400 and 200 h <sup>-1</sup> , respectively, without significant leaching of catalyst or ionic liquid. Additionally, characterization of these systems by means of FTIR, BET and XPS led to the conclusion that the presence of the metal catalyst substantially changes the IL homogeneous structure.
<i>Keywords:</i> SILP Fe(II) PNP complex Hydrogenation Ionic Liquid structure	

## 1. Introduction

Carbonyl groups and in particular their catalytic reduction using diatomic hydrogen represents a way to obtain valuable alcohols used for the manufacture of bulk and fine chemicals [1]. The selective hydrogenation of aldehydes over other carbonyl compounds remained a main challenge until last year's publication of [Fe(PNP<sup>Me</sup>-iPr)(CO)(H)(Br)] (**1**) and [Fe(PNP<sup>Me</sup>-iPr)(H)<sub>2</sub>(CO)] (**2**) as catalysts for the homogeneous chemoselective hydrogenation of aldehydes to yield alcohols [2], where TONs and TOFs up to 80,000 and 20,000h<sup>-1</sup> were achieved. Nevertheless, a major concern regarding this catalyst is the fact of being used in homogenous medium, leading to processes where fresh catalyst must be constantly added. Albeit common to almost all homogeneous processes, it is an environmental question that should be addressed.

In order to solve the aforementioned problem, ionic liquids (ILs) present themselves to be a viable solution. An IL is defined as a melting salt, having its melting point below 100°C and extremely low vapor pressure. A rough estimation points out that there must be around 10<sup>18</sup> ILs available [3]. This number results from the combination of the known anions and cations typically used for this purpose and applications on many different and exciting

fields are coming out [4,5]. Due to this myriad of possible combinations, properties of ILs range from polar to nonpolar, hydrophilic to hydrophobic, complete miscibility with water or any solvent to complete immiscibility with both. It all resumes to the appropriate choice of cation and anion; because of all this list of tuneable properties ILs are known as designer solvents [6]. A key issue though, in the search procedure for ILs, is to ensure the catalyst is stable inside the IL structure. Typically, catalysts are very sensitive to the surroundings and their deactivation is a serious problem when choosing an appropriate IL. Catalysts' properties such as nucleophilicity, Lewis acidity and basicity [7] are to be taken in consideration.

Both biphasic and supported reactions are possible solutions, which present benefits and limitations. While on the one hand biphasic reactions are easier to prepare and show better TON and TOF than supported options, leaching of both IL and catalyst is a key apprehension when considering possible scale-ups. On the other hand, supported reactions try to take out the best of heterogeneous and homogeneous reaction. In particular Supported Ionic Liquid Phase (SILP) catalysts, having received considerable attention [8], consist of a classical homogeneous catalyst dissolved in an IL and impregnated inside a porous matrix. This concept allows for an easy separation -

and subsequent recycling - when the reaction is over, without losing (or losing substantially less) catalyst and IL. All these advantages, while keeping the homogenous advantages, namely selectivity and efficiency, allow for its common classification as a green process [9].

The presence of a surface dramatically changes results based on both, homogeneous or biphasic reactions. A considerable number of publications [10,11] describe interactions between supports and the IL phase, and a communal setback

associated with SILPs is the extreme sensitivity towards surface groups, commonly leading to catalyst deactivation. Moreover, surface groups and interactions with the IL are crucial for a successful impregnation and suitable dispersion of the catalytic phase in the available surface [12].

In this work the preparation and characterization of an Fe(II) complex containing carbon based SILP used for aldehydes' selective hydrogenation, as schematically depicted in Figure 1, are presented.

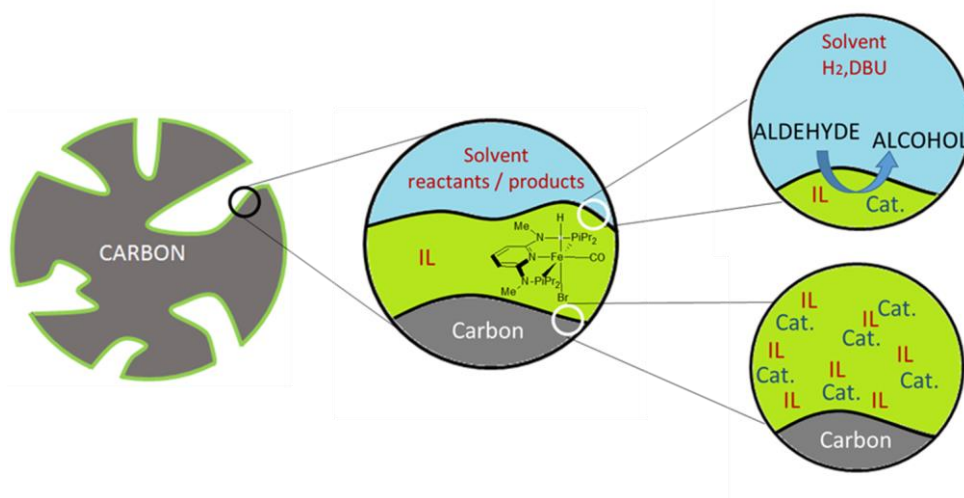


Figure 1 - Schematic representation of a carbon SILP.

## 2. Experimental

### 2.1 Materials

Activated carbon spheres were gently conceded by Blucher® Company and used after a thermal treatment at 300°C under vacuum for 24 hours.

The IL, 1-Ethyl-2,3-methylimidazolium bis(trifluoromethylsulfonyl)imide [EMMIm NTf<sub>2</sub>], was purchased from IoliTec.

All manipulations were performed under Argon atmosphere using Schlenk techniques or/and in a MBraun inert-gas glovebox. All solvents and substrates were purified according to standard procedures [13]. The deuterated solvents were purchased from Sigma-Aldrich and dried over 4 Å molecular sieves.

### 2.2 Characterization of the support/SILPs

Surface characterization of both, the support and the created SILPs were obtained using several techniques. BET method was employed (Micromeritics, ASAP 2020) at - 196°C using nitrogen as adsorption gas. Before the measurement, samples were degassed.

Regarding XPS, all measurements were carried out on a SPECS XPS-spectrometer equipped with a monochromatised Al-K $\alpha$  Xray source ( $\mu$ Focus 350) and a hemispherical WAL-150 analyser (acceptance angle: 60°). Samples were mounted onto the sample holder using double sided Cu tape or Ta. Pass energies of 100 eV and 30 eV and energy resolutions of 1 eV and 100 meV were used for survey and detail spectra respectively (excitation energy: 1486.6 eV, beam energy and spot size: 70 W onto 400  $\mu$ m, angle: 51° to sample surface

normal, base pressure:  $6 \times 10^{-10}$  mbar, pressure during measurements:  $2 \times 10^{-9}$  mbar). Data analysis was performed using CASA XPS software packages employing Shirley backgrounds [14] and Scofield sensitivity factors [15]. Charge correction was applied so the adventitious carbon peak (C-C peak) was shifted to 284.8 binding energy (BE). Curve fits using combined Gaussian-Lorentzian peak shapes were used to discern the components of detail spectra. To reduce charging effects a broad spot low energy electron source (SPECS FG 22 flood gun) was used for charge compensation (5eV/25 $\mu$ A). The detection limit in survey measurements lies around 0.1-0.5 at%, depending on the element. The accuracy of XPS measurements is around 10-20% of the values shown and the maximum depth is about 7-10 nm.

FTIR measurements were recorded with a Bruker Vertex 80 FTIR spectrophotometer using a narrow band MCT detector measuring diffuse reflectance. The scanned wavenumber range was 4000  $\text{cm}^{-1}$  to 600  $\text{cm}^{-1}$  with a resolution of 4  $\text{cm}^{-1}$  and 256 scans per spectrum. OPUS version 7.5 was the software for data analysis. The use of solid samples led to the use of potassium bromide (KBr) as the reference spectrum as well as the support to ground all the samples. The grounding was manually done for 10 minutes in order to obtain a homogeneous powder.

### 2.3 SILP manufacturing

In a flask, a mixture containing the carbon support, IL (1-Ethyl-2,3-methylimidazolium bis(trifluoromethylsulfonyl)imide) and catalyst was stirred in 2 mL of ethanol for approximately 5 minutes, under inert atmosphere. After that period, evaporation under vacuum (about  $10^{-2}$  mbar) was used in conjunction with an oil bath at 60°C until the spheres presented rolling behaviour again (about 10 minutes).

### 2.4 Hydrogenation

All hydrogenation reactions were performed in an autoclave at room temperature (25 °C), under hydrogen atmosphere between 10 and 40 bar using a 90 mL Fisher-Porter tube, which was flushed several times with hydrogen prior to use. For preparing the reaction solutions a vial was

charged with the specified amount of impregnated support and several times flushed with argon and vacuum. Subsequently, DBU, solvent and substrate were taken up into a syringe and transferred to the Fisher-Porter tube. After flushing 3 times with hydrogen, the desired pressure was established. After stirring the solution for the desired time, pressure was carefully released, and a sample for NMR was taken. If pressure was needed again, the procedure was repeated (without adding anything to the vial).

$^{19}\text{F}\{^1\text{H}\}$  NMR spectra were recorded on Bruker AVANCE-250 spectrometer controlled by Topspin and the resulting spectra were analysed using MestReNova version 6.0.2-5475. Spectra were referenced externally to  $\text{CFCl}_3$  ( $\delta = 0$  ppm).

Determination of Fe-concentrations was done using an inductively coupled plasma (ICP) optical emission spectrometer PerkinElmer OPTIMA 8300 equipped with an SC-2 DX FAST sample preparation system. A customized single-element (Merck, Roth) standard was used for the calibration. All samples were extracted using ethanol and methanol (two times each), followed by solvent-evaporation and acid-digestion ( $\text{HNO}_3$  and  $\text{H}_2\text{O}_2$  at a 2:1 ratio).

## 3. Results and Discussion

### 3.1 Surface characterization

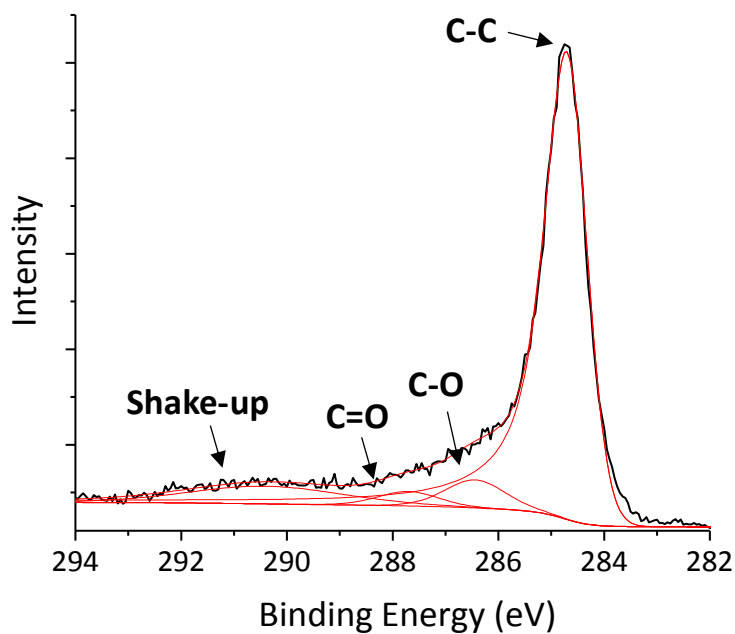
Structural parameters calculated from the  $\text{N}_2$  adsorption-desorption isotherms showed that the activated carbon spheres after thermal treatment presented a good BET surface and pore volume, with a 50:50 distribution of micro and mesopores (Table 1), compatible with catalytic applications. Furthermore the carbon spheres have an average size of 0.45  $\mu\text{m}$ .

Table 1 - BET results.

Sample	BET surface area ( $\text{m}^2/\text{g}$ )	Pore volume ( $\text{cm}^3/\text{g}$ )
Carbon	1,728	1.18

XPS measurements are able to provide evidence on surface composition. Figure 2 presents C 1s spectra of a pristine carbon sample. Quantification is possible by integration of the assigned peaks; C-C accounts for 78 % (at.), C-O, C=O, and the shake-up account for 7, 4 and 11 %, respectively. Functional groups, typically found in

carbon surfaces like phenols, ketones or pyrenes [12] are able to justify these results.



**Figure 2** – C1s spectra of a pristine carbon surface sample; black line represents experimental data and red lines the used fittings.

### 3.2 SILP characterization

The optimal determined conditions for these SILP systems are: 100 mg support, 50  $\mu\text{L}$  of IL ( $\alpha = 40\%$ ) and 5 mg of catalyst. This material is referred as CARB 40.

#### 3.2.1 FTIR measurements

Infrared measurements constitute a way of assessing the impregnation step and draw possible assumptions on whether, and how, does the IL and catalyst interact with each other and with the support itself. Being a vibrational spectroscopy, the information provided is on molecular bonds. Samples of pure ionic liquid, catalyst and CARB 40 were analysed. The results are depicted in Figure 3

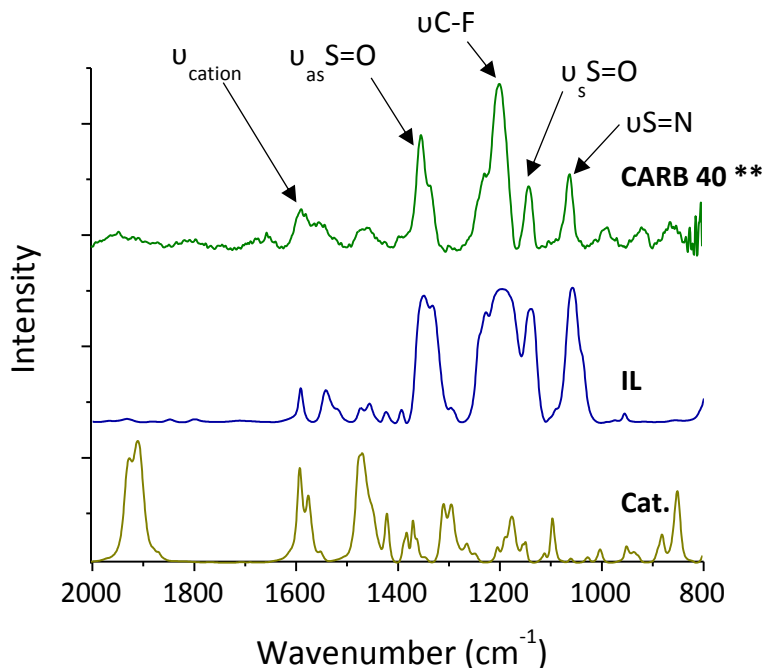


**Figure 3** – FTIR results of IL, catalyst and CARB 40. \*\*results from subtracting Carbon spectrum from CARB 12 spectrum. The spectra were baseline corrected.

The results clearly point for a successful impregnation of the IL and IL+Cat. inside the porous structure, since characteristic peaks of IL can be seen in the spectrum of CARB40, Figure 3. The strong peaks between 1400 and 1000  $\text{cm}^{-1}$  are related to the vibrations of the anion. The peak at 1054  $\text{cm}^{-1}$  is assigned to the S=N stretch, the vibration at 1190  $\text{cm}^{-1}$  corresponds to the C–F stretch, while the bands at 1350 and 1140  $\text{cm}^{-1}$  belong to the asymmetrical and symmetrical S=O stretching vibration, respectively. The peaks between 1600 and 1400  $\text{cm}^{-1}$  are related to the cation as N–C–H and H–C–H vibrations [16]. However, the peaks of the catalyst are fairly seen when the catalyst is present in the impregnation medium, since its amount is 20 and 15 times lower than the support and IL respectively.

### 3.2.2 BET measurements

Table 2 provides BET measurements not only for the pure carbon support but also for carbon impregnated with IL and CARB 40. The amounts used were always 100 mg of support, 50  $\mu\text{L}$  of IL and 5 mg of catalyst. Concerning the preparation of both impregnated samples, the procedure was

exactly the same but for the fact that one contains catalyst.

**Table 2** – BET measurements on different support stages.

Sample	BET surface area ( $\text{m}^2/\text{g}$ )	Pore volume ( $\text{cm}^3/\text{g}$ )	Theoretical Pore filling (%)	Real Pore Filling (%)
Carbon	1,728	1.18	-	-
Carbon+IL	292	0.34	40	72
CARB 40	177	0.24	40	80

Both, BET surface area and the pore volume, decreased after IL impregnation. The pore filling degree ( $\alpha$ ) defined as the volume of IL/ pore volume of carbon was calculated theoretically and experimentally. The latter value is higher, as expected, due to clogging of the pores. However, the catalyst present is not innocuous concerning the effective pore volume. CARB 40, while presenting the same theoretical pore volume, shows a higher real pore filling in addition to a decrease in surface area. It seems that, when the catalyst is solubilized, the IL layer expands to accommodate the foreign specie. A possible model already described in the literature [8,17,18],

accounts for a “cage” surrounding the metal center. It is likely that this internal structure leads to a volume expansion. In this way the catalyst promotes a conformational change in the IL structure and/or affects the viscosity and density of IL. Moreover the confinement and its effect on viscosity and density may also have influence in the presented results [19].

### 3.2.3 XPS measurements

Figure 4 shows C1s and N1s spectra for the major samples involved, as well as the structure of the IL used for the hydrogenation reactions.

Concerning the IL, in C 1s region, a set of peaks are observed; the C 1s peak at the highest binding energy, that is, at 292.7 eV, is labelled as CF<sub>3</sub> in Figure 4 – (a). It arises from the two CF<sub>3</sub> groups of the [NTf<sub>2</sub>]<sup>-</sup> anion, corroborating previous results [20,21]. These carbon atoms are the most electropositive due to covalent bonding to fluorine atoms (electron withdrawing by nature) and were fitted accordingly. The carbon signals at lower binding energies are assigned to the imidazolium ring, where carbon atoms exist with different chemical environments. A classification and deconvolution of the peaks is presented as well in Figure 4, with carbons labelled from C<sup>1</sup> to C<sup>5</sup>

according to their chemical environment. The C<sup>1</sup>:C<sup>2</sup>:C<sup>3</sup>:C<sup>4</sup>:C<sup>5</sup> ratio obtained is 1:2:2.5:1.25:1.25, which is in line with the theoretical ratio of 1:2:2:1:1. Furthermore the experimental ratio CF<sub>3</sub>:C<sup>3</sup> is 1:1 in perfect agreement with theoretical expectations.

C 1s spectra contain more information, in particular for IL+Cat. and CARB 40. In the former, the dissolution of the catalyst is clear, once CF<sub>3</sub> peak intensity is decreased. In truth this peak comes only from the IL structure, and so the increase in other Binding Energies is due to the catalyst dissolution and interaction. Concerning the latter, and comparing with the pure Carbon spectrum, the impregnation step was successful, meaning that indeed the IL and the catalyst were able to penetrate inside the porous structure.

N 1s spectra (Figure 5-(b)) emphasize the success of the impregnation. On the one hand the IL spectrum shows both cation and anion peaks, in the ratio 2:1, which is compatible with the IL structure. The dissolution of the catalyst changes this ratio to 1.1:1, once the catalyst contributes with 3 nitrogen atoms. For CARB 40 the ratio is roughly 2:1; this result shows a successful impregnation albeit the catalyst amount being under the detection limit of XPS.

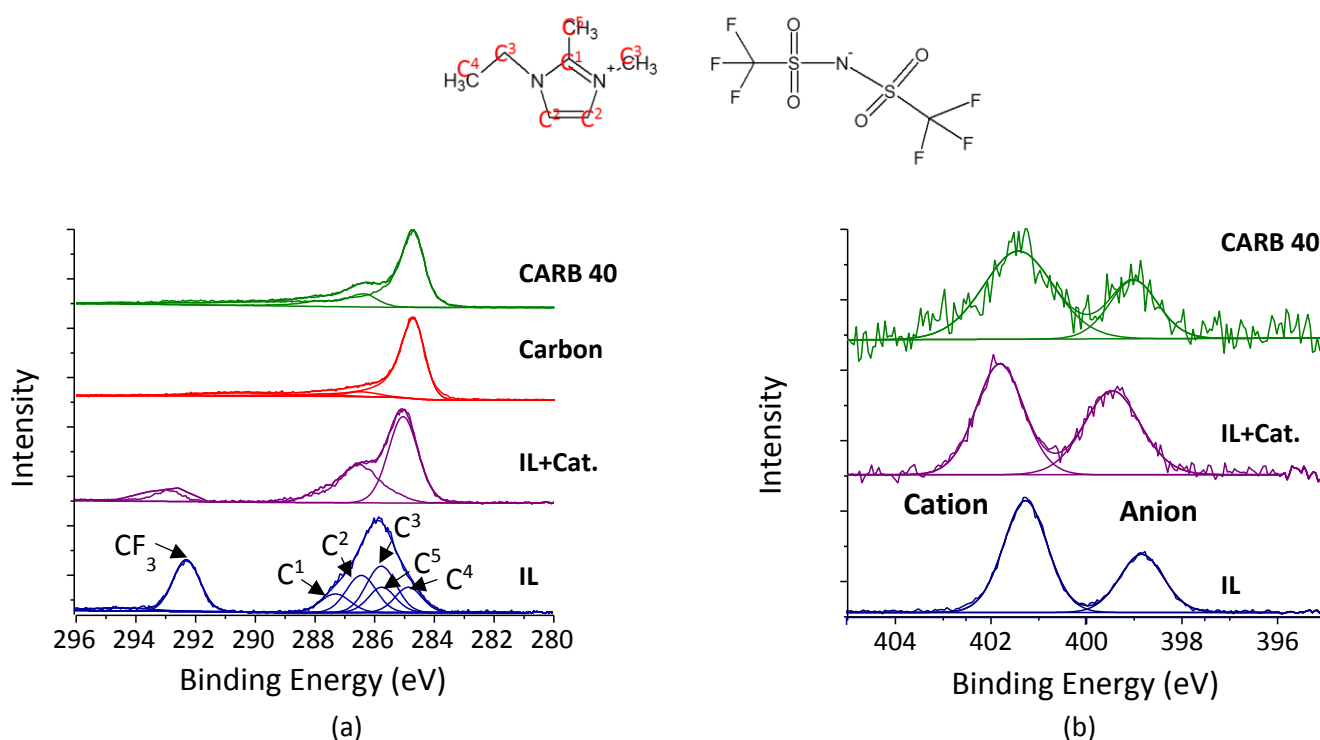
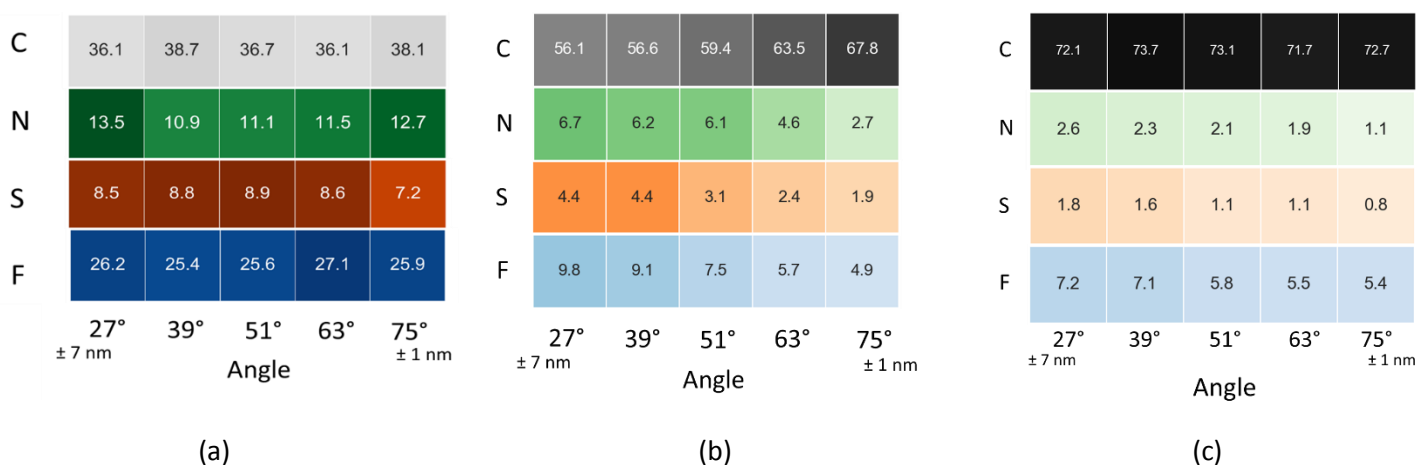


Figure 4 – XPS results for (a) C 1s spectra with IL structure and peak assignment and (b) N 1s; measurements at 51° relative to sample surface normal.

A curious and important insight comes from analysing angle dependent XP spectra, namely those corresponding to the main elements (C,N,S,F) in 3 different scenarios (Figure 5); in here the effect of catalyst dissolution in the IL matrix and consequent impregnation are highlighted. Figure 5-(a) shows a homogenous distribution of all the elements inside the pure IL structure; however, the catalyst presence (Figure 5-(b)) clearly shows a preferential arrangement of both anion and cation of the IL structure, with higher amounts of Nitrogen, Sulfur and Fluorine in deeper pores' regions. This scenario is again compatible with previous reports [17,8,18], where organometallic complexes when dissolved in IL are quickly surrounded by ion pairs of the IL (similar to solvation) forming a "cage" that traps the active catalyst. This prevents association between metal centres and obviously stabilizes the catalytic specie. This trend can be observed for CARB 40 as well ( Figure 5-(c)), although with a less pronounced degree, due to the lower relative amount of catalyst

when compared to the overall mass; a change in elemental distribution is in this way possible to infer and in line with reports pointing for an IL conformational adaption to the surface [22]. Furthermore, Figure 5-(b), presents a higher atomic percentage of carbon than what would be predictable by linear combination of IL and catalyst. This results suggest essentially a catalyst predominance in the surface region (up to 10 nm), as depicted by the higher values, associated with reported XPS carbon contamination of samples that depend on the surface cleaning method [23].

In summa, it could be pointed from XPS data that the impregnation was deemed successful and that the IL structure, with catalyst alone and/or inside the porous structure (SILP), is totally heterogeneous, due to several interactions, ranging from electrostatic and Van der Waals forces to capillary and adsorption interactions.



**Figure 5** - XPS angle dependant results for (a) IL, (b) IL+Cat., (c) CARB 40; values in atomic percentage.

### 3.3 Hydrogenations

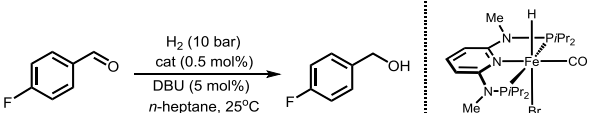
As previously described [2], the first step of the catalytic cycle is the activation of catalyst **1** to form a mixture of *cis*- and *trans*-dihydride complexes **2**, with the latter being the catalytically active species. Table 3 shows conversion values for homogeneous, biphasic and SILP systems. In a homogeneous scenario, ethanol is the reaction solvent, in accordance with the need for a protic

solvent. However, in the SILP catalyst the ionic liquid has the ability to replace ethanol as reaction medium.

From all the successful SILPs performed using activated carbon spheres, the best results are the ones with 40% (in volume) theoretical pore filling degree. Higher values are thought to clog the pores leading to a drastic decrease in surface area, and subsequently to lower conversion. For lower pore fillings, catalyst full dissolution is not possible,

leading to a situation where the catalyst is particulate.

**Table 3** - Conversion, TON and TOF values obtained for the homogeneous, biphasic and SILP system<sup>a</sup>



Condition	S/C	P (bar)	time (min)	Conversion (%)	TON	TOF (h <sup>-1</sup> )
homogeneous	200	10	7	>99	200	1714
biphasic	200	10	60	> 99	200	200
CARB 25	200	10	180	6	12	4
CARB 30	200	10	180	8	16	5
<b>CARB 40</b>	<b>200</b>	<b>10</b>	<b>180</b>	<b>&gt; 99</b>	<b>200</b>	<b>67</b>
CARB 50	200	10	180	22	44	15
CARB 60*	200	10	120	> 99	200	100
CARB 25	200	40	180	> 99	200	67
CARB 30	200	40	180	> 99	200	67
CARB 40	200	40	120	> 99	200	100
CARB 50	200	40	150	> 99	200	80
CARB 60*	200	40	90	> 99	200	133
CARB 40	200	20	120	> 99	200	100
CARB 40	200	30	120	> 99	200	100
CARB 40	400	10	150	20	80	32
<b>CARB 40</b>	<b>400</b>	<b>40</b>	<b>120</b>	<b>&gt; 99</b>	<b>400</b>	<b>200</b>
CARB 40	1000	10	300	20	200	40
CARB 40	1000	40	180	22	220	73

\* - leaching of IL detected by <sup>19</sup>F NMR

<sup>a</sup> - Experimental conditions: 2-10 mmol of substrate, 100 mg of carbon support, 5 mg of catalyst, 45-105 mg of IL, 5 mol% of DBU, 2 mL of heptane, 25 °C

Substrate to catalyst (S:C) ratio can go up to 400, keeping up with the same values of conversion found for S:C = 200. TON and TOF values for supported reactions are more modest than those of homogenous and biphasic, in accordance with mass transfer limitations experienced in the SILP, mainly caused by hydrogen solubility as well as the migration of both substrate and product to/from the IL matrix. Iron leaching, measured by ICP-MS, was below 0.177±0.008 mol% with respect to the initial loading.

SILP recyclability was tested with a considerable loss of activity in subsequent hydrogenations. This catalyst deactivation is associated with the interruption of the catalytic

cycle due to lack of substrate. Nevertheless, implementation in a continuous reactor seems promising.

#### 4. Conclusions

SILP catalysis has a lot to offer to both academic and industrial applications. In the present work a successful SILP system was created for the hydrogenation of aldehydes, comprising mesoporous activated carbon spheres, an Fe(II) PNP pincer complex catalyst and an imidazolium based IL. We characterized the support, which was used without any chemical modification, and the SILP via combining FTIR, BET and XPS measurements. The best SILP system was catalytically active under mild conditions, without significant leaching of IL or catalyst. Moreover, it showed the promise of becoming an efficient catalyst under continuous flow conditions. In addition, it seems that the catalyst is changing dramatically the IL structure and affecting the overall system which is an interesting result to be used in future work.

#### References

- Johnson, N. B., Lennon, I. C., Moran, P. H. & Ramsden, J. A. Industrial-scale synthesis and applications of asymmetric hydrogenation catalysts. *Acc. Chem. Res.* **40**, 1291–1299 (2007).
- Gorgas, N., Stöger, B., Veiros, L. F. & Kirchner, K. Highly Efficient and Selective Hydrogenation of Aldehydes: A Well-Defined Fe(II) Catalyst Exhibits Noble-Metal Activity. *ACS Catal.* **6**, 2664–2672 (2016).
- Carmichael, A. J. & Seddon, K. R. Polarity study of some 1-alkyl-3-methylimidazolium ambient-temperature ionic liquids with the solvatochromic dye, Nile Red. *J. Phys. Org. Chem.* **13**, 591–595 (2000).
- Cevasco, G. & Chiappe, C. Are ionic liquids a proper solution to current environmental challenges? *Green Chem.* **16**, 2375 (2014).
- Smiglak, M. *et al.* Ionic liquids for energy, materials, and medicine. *Chem. Commun.* **50**, 9228–9250 (2014).
- Plechkova, N. V. & Seddon, K. R. Ionic Liquids: 'Designer' Solvents for Green Chemistry. *Methods Reagents Green Chem. An Introd.* **2000**, 103–130 (2007).
- Corma, A. & Garcia, H. Lewis acids: From conventional homogeneous to green homogeneous and heterogeneous catalysis. *Chem. Rev.* **103**, 4307–4365 (2003).
- Fehrmann, R., Riisager, A. & Haumann, M. *Supported Ionic Liquids - Fundamentals and Applications*. (Wiley-VCH, 2014).



9. García-Verdugo, E., Altava, B., Burguete, M. I., Lozano, P. & Luis, S. V. Ionic liquids and continuous flow processes: a good marriage to design sustainable processes. *Green Chem.* **17**, 2693–2713 (2015).
10. Lemus, J., Palomar, J., Gilarranz, M. A. & Rodriguez, J. J. Characterization of Supported Ionic Liquid Phase (SILP) materials prepared from different supports. *Adsorption* **17**, 561–571 (2011).
11. Yu, N. *et al.* Gold nanoparticles supported on periodic mesoporous organosilicas for epoxidation of olefins: Effects of pore architecture and surface modification method of the supports. *Microporous Mesoporous Mater.* **143**, 426–434 (2011).
12. Shafeeyan, M. S., Daud, W. M. A. W., Houshmand, A. & Shamiri, A. A review on surface modification of activated carbon for carbon dioxide adsorption. *J. Anal. Appl. Pyrolysis* **89**, 143–151 (2010).
13. Armarego, W. L. . & Perrin, D. . *Purification of Laboratory Chemicals*. (4th ed.; Pergamon: New York, 1997).
14. Shirley, D. A. High-resolution x-ray photoemission spectrum of the valence bands of gold. *Phys. Rev. B* **5**, 4709–4714 (1972).
15. Scofield, J. H. Hartree-Slater subshell photoionization cross-sections at 1254 and 1487 eV. *J. Electron Spectros. Relat. Phenomena* **8**, 129–137 (1976).
16. Dong, K., Zhao, L., Wang, Q., Song, Y. & Zhang, S. Are ionic liquids pairwise in gas phase? A cluster approach and in situ IR study. *Phys. Chem. Chem. Phys.* **15**, 6034 (2013).
17. Sievers, C., Jimenez, O., Müller, T. E., Steuernagel, S. & Lercher, J. A. Formation of solvent cages around organometallic complexes in thin films of supported ionic liquid. *J. Am. Chem. Soc.* **128**, 13990–13991 (2006).
18. Fow, K. L., Jaenicke, S., Müller, T. E. & Sievers, C. Enhanced enantioselectivity of chiral hydrogenation catalysts after immobilisation in thin films of ionic liquid. *J. Mol. Catal. A Chem.* **279**, 239–247 (2008).
19. Singh, M. P., Singh, R. K. & Chandra, S. Ionic liquids confined in porous matrices: Physicochemical properties and applications. *Prog. Mater. Sci.* **64**, 73–120 (2014).
20. Höfft, O. *et al.* Electronic structure of the surface of the ionic liquid [EMIM][Tf 2N] studied by metastable Impact Electron Spectroscopy (MIES), UPS, and XPS. *Langmuir* **22**, 7120–7123 (2006).
21. Smith, E. F., Rutten, F. J. M., Villar-Garcia, I. J., Briggs, D. & Licence, P. Ionic liquids in vacuo: Analysis of liquid surfaces using ultra-high-vacuum techniques. *Langmuir* **22**, 9386–9392 (2006).
22. Steinrück, H. P. *et al.* Surface science and model catalysis with ionic liquid-modified materials. *Adv. Mater.* **23**, 2571–2587 (2011).
23. Taylor, C. E., Garvey, S. D. & Pemberton, J. E. Carbon Contamination at Silver Surfaces: Surface Preparation Procedures Evaluated by Raman Spectroscopy and X-ray Photoelectron Spectroscopy. *Anal. Chem.* **68**, 2401–2408 (1996).